# Two Fluid Flow in a Capillary Tube

**Melissa Strait, Michael Shearer, Rachel Levy, Luis Cueto-Felgueroso, and Ruben Juanes**

## 1 Model

The displacement of a fluid such as water by an injected finger of air in a narrow tube is a classic problem of fluid mechanics. Since the early experimental and theoretical work of Bretherton [4] and Taylor [10], there has been much research on the injection of one fluid into a different fluid resident in a thin tube [1, 3, 6, 7]. Characterizing such flows is significant not only for small scale fluid devices but also for modeling macroscopic two fluid flow in porous media [3, 9]. In this paper, we consider a recent model [5] that incorporates ideas from phase field theory, resulting in a fourth order nonlinear partial differential equation (PDE) similar to the PDE of thin liquid films [2]. The PDE possesses a spinodal-type instability at long wavelengths that we associate with the physical varicose or Plateau instability, in which the cylindrical gas finger, of sufficient length and for a range of widths, tends to break up into bubbles [7, 8].

We consider an axisymmetric flow of air displacing water in a cylindrical capillary tube. The dependent variable, which we refer to as the saturation $u$, is the cross-sectional area fraction of gas. The PDE model considered in [5] neglects the effect of gravity (which is reasonable for a thin tube, but can have a significant effect in wider tubes [7]) and takes the form

M. Strait • M. Shearer (✉)
Department of Mathematics, North Carolina State University, Raleigh, NC 27695, USA
e-mail: melissa.strait@gmail.com; shearer@ncsu.edu

R. Levy
Department of Mathematics, Harvey Mudd College, Claremont, CA 91711, USA

L. Cueto-Felgueroso • R. Juanes
Department of Civil and Environmental Engineering, Massachusetts Institute of Technology, Cambridge, MA 02139, USA



J. Rychtář et al. (eds.), *Collaborative Mathematics and Statistics Research*, Springer Proceedings in Mathematics & Statistics 109, DOI 10.1007/978-3-319-11125-4_14

$$\partial_t u + \partial_x f(u) = \partial_x \left( f(u)\lambda(u)\frac{1}{Ca}\partial_x \psi \right). \tag{1}$$

In this equation, the gas saturation $u = u(x,t)$ depends on $x$, the distance along the length of the tube and time $t$. The flux function $f$ is the fractional flow rate, given by

$$f(u) = \frac{u}{u + k_w(u)},$$

and depends on the relative permeability $k_w(u)$ of water, which we take as either $k_w(u) = (1-u)^3$, or $k_w(u) = (1-u)^4$. We write $\lambda(u) = k_w(u)\frac{1}{M}(1 + (M-1)u)$, in which the mobility number $M = \eta_w/\eta_g > 1$ is the ratio of the viscosities $\eta_w, \eta_g$ of the two fluids. The capillary number $Ca = U\eta_w/\gamma$ is the ratio of viscous and capillary forces, depending on $U$, a typical finger tip velocity, and $\gamma$, the surface tension between the two fluids. The function

$$\psi = C_1 g(u) - C_2\sqrt{\kappa(u)}\partial_x\left(\sqrt{\kappa(u)}\partial_x u\right),$$

is the chemical potential, derived as the variational derivative of a total free energy $F(u, \partial_x u)$. This has the form $F(u, \partial_x u) = C_1 F_0(u) + C_2\kappa(u)(\partial_x u)^2$, representing a bulk free energy plus an interface free energy. For simplicity in this paper, we take the bulk free energy to be a double-well quartic function of $u$, with

$$g(u) = u(1-u)(1-2u) = F_0'(u);$$

we generally take the coefficient of interfacial energy $\kappa(u)$, which is quadratic as $u \to 0$, to be $\kappa(u) = u^2$, as in [5]. The parameters $C_1, C_2$ are positive, and can be chosen so that the model accommodates the Young–Laplace law for the contact line at the tube entrance, where the gas finger attaches to the tube wall.

The objective of this paper is to outline a preliminary analysis of gas finger solutions of the PDE (1). These are traveling waves with the unusual property of being of finite extent, terminating at the tip of the gas finger in Fig. 1. Such traveling waves are solutions of a third order ordinary differential equation that is singular at the tip, where $u = 0$. With a change of variables, we transform the singular equation into a system that has a regular equilibrium at $u = 0$, and allows the numerical simulation of traveling waves. However, the solutions are not structurally stable, and depend on varying a parameter, specifically the finger width. Consequently, for each capillary number $Ca$ in a specified range, there is a unique upstream width

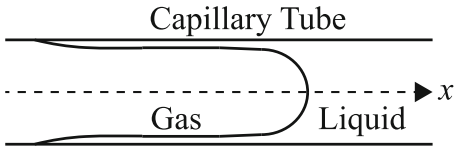


**Fig. 1** Schematic of a gas finger displacing a liquid in a capillary tube

corresponding to a traveling wave. The range for $Ca$ is determined by the nature of the equilibrium at $u = 0$, to avoid unphysical oscillations, since the saturation $u$ has to remain non-negative. These properties are established in Sect. 2. In Sect. 3, we describe PDE simulations using a finite difference code, and compare the results to the traveling wave calculations and to experimental results of Taylor [10]. In the short Sect. 4, we describe the varicose instability by linearizing the PDE about a constant width finger. Finally, the results are discussed in Sect. 5.

## 2 Traveling Waves

In experiments, it is observed that the spherical tip of the gas finger travels with constant speed, and as the finger elongates, it leaves behind a nearly uniform layer of fluid adjacent to the tube wall [10]. To capture this behavior analytically, we seek traveling wave solutions $u(x,t) = u(x - st)$ of the PDE (1), where $s$ is the wave speed. Such a solution has $u = 0$ at the tip of the gas finger. By translation invariance of the problem, we take this location to be $x = st$, without loss of generality. If $u_L > 0$ is the thickness of the fluid layer behind the tip, mathematically, the saturation should approach $u_L$ as $\xi = x - st \to -\infty$. In summary, we have boundary conditions

$$u(-\infty) = u_L, \quad u(0) = 0. \tag{2}$$

Consistent with a smooth tip of the gas finger, we shall also assume that derivatives of $u$ are bounded as $\xi \to 0$. Moreover, derivatives of $u(\xi)$ are taken to approach zero as $\xi \to -\infty$.

Substituting $u = u(\xi)$, $\xi = x - st$ into (1) and integrating once, we obtain the third order ODE

$$K - su + f(u) = f(u)\lambda(u)\frac{1}{Ca}\psi', \quad \psi = C_1 g(u) - C_2\sqrt{\kappa(u)}\left(\sqrt{\kappa(u)}u'\right)',$$

where $K$ is the constant of integration. Enforcing the boundary conditions at $\xi = 0, \xi = -\infty$, we find that $K = 0$, and that the speed $s$ is given by the Rankine–Hugoniot condition

$$s = \frac{f(u_L)}{u_L}.$$

Incidentally, these conclusions depend on the degeneracy at $u = 0$, specifically that $f(0) = 0$. Now we have the ODE

$$\begin{aligned} -su + f(u) &= \frac{1}{Ca}C_1 H(u)\frac{dg(u)}{du}u' - C_2\frac{1}{Ca}H(u)\left(\sqrt{\kappa}(\sqrt{\kappa}u')'\right)', \\ H(u) &= f(u)\lambda(u). \end{aligned} \tag{3}$$

Equation (3) can be written as a first order system:

$$\begin{aligned}\sqrt{\kappa}u'(\xi) &= v\\ \sqrt{\kappa}v'(\xi) &= w\\ \sqrt{\kappa}w'(\xi) &= \frac{C_1}{C_2}G(u)v + \frac{Ca\sqrt{\kappa(u)}}{C_2H(u)}(su - f(u)),\end{aligned} \tag{4}$$

where $G(u) = \frac{dg(u)}{du}$. Since $\kappa(u) \sim u^2$ as $u \to 0$, system (4) has a singularity at $u = 0$. To remove the singularity, we introduce a new independent variable $\eta$. If $(u(\xi), v(\xi), w(\xi))$ is a traveling wave solution of (4), we set

$$\sqrt{\kappa(u(\xi))}\frac{d}{d\xi} = \frac{d}{d\eta},$$

and let $U(\eta) = u(\xi)$, $V(\eta) = v(\xi)$, $W(\eta) = w(\xi)$. For convenience, we revert to the lowercase letters, with $u(\eta)$, etc. Then, with $' = \frac{d}{d\eta}$,

$$\begin{aligned}u'(\eta) &= v\\ v'(\eta) &= w\\ w'(\eta) &= \frac{C_1}{C_2}G(u)v + \frac{Ca\sqrt{\kappa(u)}}{C_2H(u)}(su - f(u)).\end{aligned} \tag{5}$$

Now $H(u) = f(u)\lambda(u) \sim \frac{1}{M}u$, and $\sqrt{\kappa(u)} \sim u$, so the vector field represented by the right-hand side of Eq. (5) has a regular equilibrium at $u = 0$. Consequently, we seek trajectories $(u(\eta), v(\eta), w(\eta))$ from $(u_L, 0, 0)$ (as $\eta \to -\infty$), to $(0, 0, 0)$ (as $\eta \to +\infty$) with the property that $u$ remains non-negative.

## 2.1 Equilibria

The system (5) has equilibria when $(u', v', w') = (0, 0, 0)$. Then $v = w = 0$, and equilibrium values of $u$ are solutions of $su - f(u) = 0$, the intersection points of the flux function graph $y = f(u)$, and the line $y = su = \frac{f(u_L)}{u_L}u$. These curves necessarily intersect at $u = 0$ and $u = u_L$. Let $u^*$ be defined as the value of $u$ for which the tangent to the graph of $f$ passes through the origin, shown in Fig. 2:

$$\frac{f(u^*)}{u^*} = f'(u^*).$$

A simple calculation shows that $u^* = 1 - 1/\sqrt{3}$. Let $s^* = (u^* + (1 - u^*)^3)^{-1}$ be the corresponding speed. For $u^* < u_L < 1$, there is a middle equilibrium $u_M$ such that $0 < u_M \leq u^* < u_L$. Since $f(u) \sim u$ near $u = 0$, we observe that $u_M \to 0$ as $u_L \to 1$.

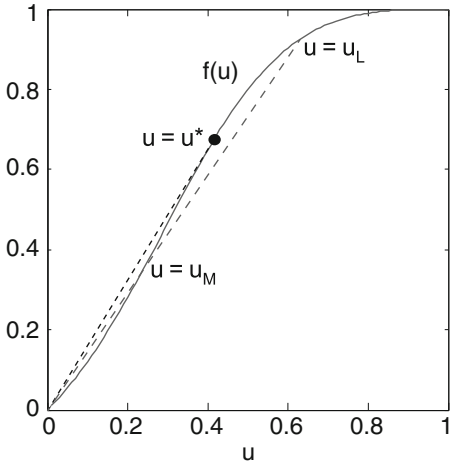


**Fig. 2** Graph of the flux function $f(u)$, showing $u^*$ and possible equilibrium values $u = u_L, u_M$ with the same $s = f(u_L)/u_L$

## 2.2 A Necessary Condition for Non-negative Traveling Waves

To obtain physically relevant solutions, in which the saturation $u$ remains positive, we determine a bound on the quantity $M \cdot Ca$ by analyzing the linearized system at $(0, 0, 0)$. Recall that near $u = 0$,

$$H(u) = f(u)\lambda(u) = \frac{u(1-u)^3}{u + (1-u)^3}\frac{1}{M}(1 + (M-1)u) \sim \frac{1}{M}u,$$
$$f'(0) = 1, \quad \text{and} \quad G(0) = 1.$$

Therefore, system (5) linearized around $u = v = w = 0$ has the structure

$$\begin{bmatrix} u' \\ v' \\ w' \end{bmatrix} = \begin{bmatrix} 0 & 1 & 0 \\ 0 & 0 & 1 \\ \frac{MCa}{C_2}(s-1) & \frac{C_1}{C_2} & 0 \end{bmatrix} \begin{bmatrix} u \\ v \\ w \end{bmatrix}.$$

The nature of the equilibrium at the origin is determined by the eigenvalues $\lambda_k$, $k = 1, 2, 3$ of the coefficient matrix. These are the three roots of the function

$$y(\lambda) = \lambda^3 - \frac{C_1}{C_2}\lambda - \frac{Ca}{C_2}M(s-1). \tag{6}$$

Note that the $\lambda_1\lambda_2\lambda_3 = \frac{Ca}{C_2}M(s-1) > 0$, and $\lambda_1 + \lambda_2 + \lambda_3 = 0$. Consequently, one eigenvalue is positive and the other two are either negative or are complex conjugates and have negative real parts. The latter eigenvalues correspond to the two-dimensional stable manifold of the equilibrium at the origin, on which the

desired trajectory must lie. In order to prevent the gas saturation, $u$ on this manifold from becoming negative, all three eigenvalues must be real, since otherwise solutions will have oscillations around $u = 0$, and $u$ will not remain positive.

To determine the range of parameters for which all three eigenvalues are real, we analyze the function $y(\lambda)$ in (6). The local maximum, $y(\lambda_m)$, occurs at $\lambda_m = -\sqrt{\frac{C_1}{3C_2}}$.

There are three real roots when $y(\lambda_m) > 0$, leading to the following lemma.

**Lemma 1** *Suppose there is a traveling wave solution of* (1)*, satisfying* (2) *with* $u \geq 0$.

(a) *Then*

$$M \cdot Ca < \frac{2}{3\sqrt{3}(s-1)} \sqrt{\frac{C_1^3}{C_2}}, \tag{7}$$

*where* $s = f(u_L)/u_L$.

(b) *Suppose moreover, that* $\overline{s} > 1$ *is defined by*

$$M \cdot Ca = \frac{2}{3\sqrt{3}(\overline{s}-1)} \sqrt{\frac{C_1^3}{C_2}}.$$

*Then* $s < \min(\overline{s}, s^*)$.

The implication of part (b) is that if $\overline{s} < s^*$, then the possible range of values of the traveling wave speed $s$ is restricted, and consequently, the possible values of $u_L$ are also restricted. Specifically, let $\overline{u}_L$ be defined by $\overline{s} = f(\overline{u}_L)/\overline{u}_L$. Then in order that $1 < s < \overline{s}$, we must have $\overline{u}_L < u_L < 1$.

## 2.3 The Equilibrium at $u_L > 0$

Since $H(u_L) > 0$, the equilibrium at $u = u_L$ is regular, and the Jacobian of $F$ is given by

$$DF(u_L, 0, 0) = \begin{bmatrix} 0 & 1 & 0 \\ 0 & 0 & 1 \\ \frac{Ca\sqrt{\kappa(u_L)}}{C_2 H(u_L)}(s - f'(u_L)) & \frac{C_1}{C_2} G(u_L) & 0 \end{bmatrix}.$$

The characteristic polynomial associated with this system is

$$y(\lambda) = \lambda^3 - A\lambda - B,$$

where $A = \frac{C_1}{C_2} G(u_L)$, and $B = \frac{u_L Ca}{C_2 H(u_L)}(s - f'(u_L))$. The eigenvalues, given by the zeroes of $y(\lambda)$, vary continuously with the coefficients $A, B$. For $A = 0$, the three eigenvalues are (complex) cube roots of $B$. Consequently, if $u_L > u^*$, then $B > 0$, and there is one positive real eigenvalue, and a pair of complex conjugate eigenvalues with negative real parts.

If an eigenvalue crosses the imaginary axis as $A$ is varied, then for some $A$, the real part of the eigenvalue vanishes, so $\lambda = i\beta$, $\beta \in \mathbb{R}$. Therefore,

$$y(\lambda) = -i\beta^3 - Ai\beta - B = 0,$$

a contradiction. We conclude that, for $u_L > u^*$, two eigenvalues of the equilibrium at $u_L$ have negative real parts, and the third eigenvalue is real and positive. Consequently, the local dynamics are described by a two-dimensional stable manifold and a one-dimensional unstable manifold at $u_L$. Similarly, if $0 < u_L < u^*$, the equilibrium at $u_L$ has a two-dimensional unstable manifold and a one-dimensional stable manifold, since in that case, we have $s < f'(u_L)$ and $B < 0$.

Finally, we observe from the structure of $DF(u)$ that right eigenvectors have the form $(1, \lambda, \lambda^2)^T$, for each eigenvalue $\lambda$ of $DF(u)$.

## 2.4 Computing the Traveling Wave Solutions

We seek a solution of system (5) that connects $(u_L, 0, 0)$ to $(0, 0, 0)$ with $u_L > u^*$. Such a solution corresponds to a trajectory that leaves $(u_L, 0, 0)$ on its one-dimensional unstable manifold $W^U(u_L)$, and intersects the two-dimensional stable manifold $W^S(0)$ of the equilibrium at $u = 0$. Then the entire trajectory lies in $W^S(0)$. However, this intersection has to be achieved by varying a parameter, suggesting a shooting method. Geometrically, the intersection is codimension one. In this sense, the corresponding traveling wave solutions of (1) are undercompressive, as discussed in [2].

Let the parameters $Ca$ and $M$ be fixed. We use an ODE solver in MATLAB to approximate the trajectory leaving $(u_L, 0, 0)$ along $W^U(u_L)$, with $u(\eta)$ decreasing. To this end, we initiate the ODE solver by taking $(u, v, w)$ a small distance $\epsilon > 0$ away from $(u_L, 0, 0)$ along the eigenvector $-(1, \lambda, \lambda^2)$, where $\lambda$ is the positive eigenvalue associated with the equilibrium at $u_L$ :

$$(u, v, w)(0) = (u_L, 0, 0) - \epsilon(1, \lambda, \lambda^2).$$

We solve the system (5) in MATLAB, and track the sign of $u(\eta)$ and $u'(\eta)$ for each choice of $u_L$. In extreme cases, the trajectory exhibits contrasting behavior, corresponding to missing $W^S(0)$ on one side or the other: (a) For $u_L$ close to $u = 1$, $u(\eta)$ becomes negative, and (b) for $u_L$ close to $u^*$, $u(\eta)$ remains positive but has a positive minimum before exceeding $u = u_L$. These two behaviors are incorporated

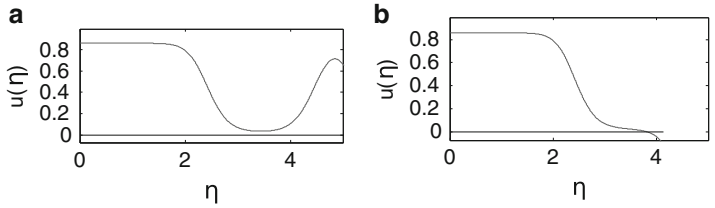


**Fig. 3** Trajectories exhibiting the two behaviors seen when using the bisection method to solve system (5). (**a**) $u(\eta) > 0$ has a minimum. (**b**) $u(\eta)$ crosses $u = 0$

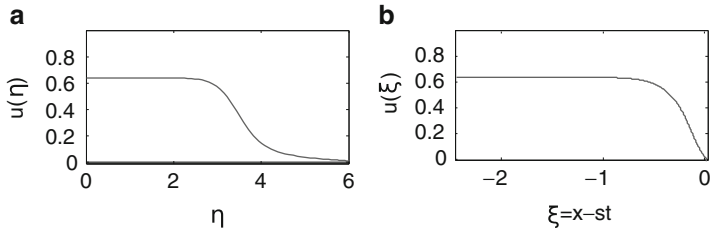


**Fig. 4** Traveling waves: (**a**) in the transformed variable $\eta$; (**b**) in the physical variable $\xi$

into an interval division algorithm (bisection method) to approximate the value of $u_L$ for which $u(\eta)$ remains positive, while its minimum is pushed off towards $\eta = \infty$.

Examples of trajectories with the two behaviors are shown in Fig. 3, and a typical trajectory $u = u(\eta)$ is shown in Fig. 4a.

As we vary the capillary number $Ca$, we find new values of $u_L = u_L(Ca)$ for which there is a trajectory from $u_L$ to $u = 0$. A plot of $1 - u_L$ against $Ca$ is shown in Fig. 6, together with comparisons to experiment and PDE simulations, as explained below.

## 2.5 *Inverting the Transformation*

The trajectories in the previous subsection were obtained in the transformed independent variable $\eta$, with a solution $\tilde{u}(\eta)$, $-\infty < \eta < \infty$. To convert back to the physical variable $\xi$, which remains finite, and derive the desired function $u(\xi)$, we first recall that the change of variables from $\xi$ to $\eta$ was predicated on the existence of a solution $u(\xi)$, so that

$$\sqrt{\kappa(u)}\frac{du}{d\xi} = \frac{d\tilde{u}}{d\eta}. \tag{8}$$

However, if the change of variables is $\eta = \eta(\xi)$, we have $\tilde{u}(\eta(\xi)) = u(\xi)$. Inverting, if $\xi = \xi(\eta)$ then from the chain rule

$$\frac{d\xi}{d\eta} = u(\xi(\eta)).$$

Solving this ODE using separation of variables gives

$$\xi = -\int_{\eta}^{\infty} \tilde{u}(\bar{\eta}) d\bar{\eta}.$$

Since we assume our traveling wave solution $u(\eta) \approx 0$ for $\eta \geq N$, for large enough $N > 0$, then

$$\xi = -\int_{\eta}^{N} \tilde{u}(\eta) d\eta.$$

The traveling wave solution with the inversion completed is shown in Fig. 4b, where we have used $\kappa(u) = u^2$ for both the ODE solver and the transformation.

### 2.6 Conclusion

For each $Ca \in [10^{-3}, 1]$ and for fixed $C_1, C_2$, and $M$ satisfying (7), the method described in Sect. 2.4 generates a unique traveling wave solution to (1) subject to (2). We conjecture, and find numerically, that for each $Ca$ and fixed $C_1, C_2$, and $M$ there is a unique $u_L$ with a traveling wave connecting $u_L$ to 0. The numerical method for finding $u_L$ for each value of $Ca$ is robust, but quite sensitive, meaning that $u_L$ has to be calculated to a large number of decimal places (around 12–14) in order to have the flat portion near $u = 0$ extend as in Fig. 4a for example.

## 3 PDE Simulations

The PDE (1) is solved using an implicit finite difference method to model the injection of a gas finger into a fluid filled tube. A fixed domain, $x \in [-L, L]$, is used with boundary conditions

$$u(-L, t) = 1, \quad u(L, t) = 0, \quad u'(-L, t) = 0, \quad u'(L, t) = 0,$$

$L$ is chosen to be large enough to assume zero gas saturation at $x = L$. Finite difference simulations in Fig. 5 show a traveling wave advancing ahead of a rarefaction wave, connected by a plateau region of residual fluid.

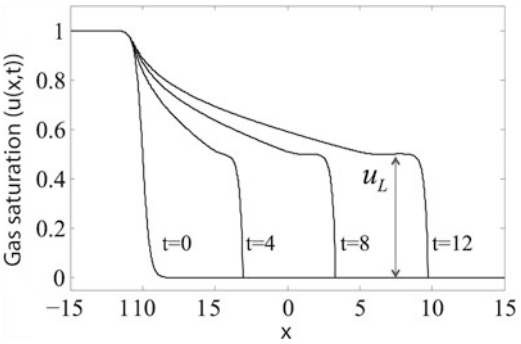


**Fig. 5** Finite difference simulations of air injection with $L = 15$, $Ca = 0.5$, $M = 10$, $C_1 = 0.2$, and $C_2 = \frac{1}{7}$

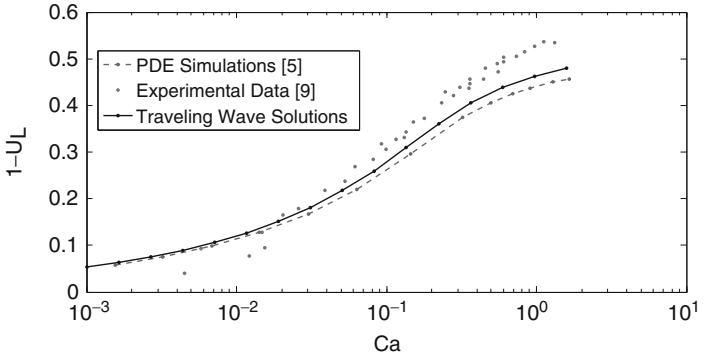


**Fig. 6** Comparison of the residual fluid remaining, $1 - u_L$, in simulations and experiments [10]

The height of the traveling wave from PDE simulations can be compared with the traveling wave height computed from the ODE (4) and results from classical experiments by Taylor. The PDE and ODE simulation data along with experimental data from [10] are shown in Fig. 6. The amount of fluid left behind, between the gas finger and tube wall, $1 - u_L$, is plotted against the capillary number, $Ca$. Both simulations and experiments show that as $Ca$ increases, the amount of fluid left increases. The PDE and ODE simulations closely agree for $Ca \in [10^{-3}, 1.5]$. Both simulations predict the same trend as the experimental data [10], but under-predict the amount of fluid remaining for large capillary numbers.

The model (1) assumes the relative permeability of the water, $\lambda_w$, has the form $\lambda_w = (1-u)^3$. The agreement between model simulations and experimental data for larger $Ca$, in the range $[10^{-1}, 1.5]$, can be improved by changing the form of $\lambda_w$ to a quartic function, $\lambda_w = (1-u)^4$. This changes $f(u)$ and $\lambda(u)$ in (1) to

$$f(u) = \frac{u}{u + (1-u)^4}, \qquad \lambda(u) = (1-u)^4 \frac{1}{M}(1 + (M-1)u).$$

Refining the choice of $C_1$ and $C_2$ can also better fit the simulations to experimental results.

## 4 Varicose Instability

The Rayleigh–Plateau instability causes long gas fingers to break into bubbles, as observed in experiments in [7]. To compare this physical instability to the stability of the PDE we analyze (1) linearized about a constant $u_0$. For $u(x,t) = u_0 + \epsilon\tilde{u}(x,t)$, with $\epsilon << 1$, the linearized PDE is

$$\tilde{u}_t + f'(u_0)\tilde{u}_x = \frac{H(u_0)}{Ca}\left(C_1 g'(u_0)\tilde{u}_{xx} - C_2 u_0^2 \tilde{u}_{xxxx}\right). \tag{9}$$

To find the dispersion relation between the frequency, $\omega(\xi)$, and wave number $\xi$, we assume a perturbation of the form $\tilde{u}(x,t) = e^{i(\xi x+\omega t)}$ and substitute into (9) resulting in

$$\omega(\xi) = -f'(u_0)\xi + i\frac{H(u_0)}{Ca}\left[C_1 g'(u_0)\xi^2 + C_2 u_0^2 \xi^4\right]. \tag{10}$$

The perturbation decays with time if and only if Im $\omega > 0$. This results in the stability restriction

$$0 < \frac{H(u_0)}{Ca}\left[C_1 g'(u_0)\xi^2 + C_2 u_0^2 \xi^4\right]. \tag{11}$$

In order for perturbations to decay for all wave numbers, $\xi$, $g'(u_0)$ must be positive. However, for the choice of nonlinearity in this paper, $g'(u) < 0$ in the range $0.212 < u < 0.788$. Thus, the solutions can be expected to develop long wave instabilities in this range.

We can also determine the wavelengths that increase in amplitude in this range of $u$. The wavelength, $\lambda$, is related to the wave number, $\xi$, by the

$$\lambda = \frac{2\pi}{\xi}.$$

To find the range of unstable $\lambda$, we determine the values of $\xi$ such that (11) is not satisfied. At $u = 0.5$, $g'(u)$ attains its minimum value, $g(0.5) = -0.5$. For definiteness, let $C_1 = 1$, $C_2 = 0.1$, values used in the simulations. Then Im $\omega < 0$ when $|\xi| \leq \sqrt{20}$. Therefore the range of unstable wavelengths in this particular case is $\lambda \geq \frac{2\pi}{\sqrt{20}} \approx 1.4$.

## 5 Discussion

In this paper, we have verified that the phase field model of [5] captures the structure of a gas finger being forced into a capillary tube filled with water. The model

PDE describes the evolution of the gas saturation assuming an axisymmetric cross-section through the gas and water. It incorporates a bulk free energy and an interfacial energy, with surface tension incorporated into a capillary number $Ca$. The structure of the PDE solution is approximately a spreading rarefaction wave attached to the tube entrance, preceded by the finger, which is a traveling wave that terminates at the finger tip. To calculate the traveling wave, we use a change of variables which sends the tip to infinity and makes the zero saturation limit at the tip a regular equilibrium for the associated ODE system.

The ODE solution has to remain positive in order to be physical, and this entails a maximum capillary number. Below this threshold, we calculate a value of the finger width (more precisely the saturation $u_L$) in the traveling wave using a shooting method. The structure of the wave is similar to that observed in driven thin liquid films, also modeled with a fourth order PDE [2]. The values of $u_L$ compare well with those observed in finite difference simulations of the PDE, and with experimental observations of Taylor [10].

In all of these comparisons, simple constitutive functions have been used, specifically, $g(u) = u(u-1)(1-2u)$, and $\kappa(u) = u^2$. The varicose instability, generated as a result of the non-monotonicity of $g(u)$, can be tuned using different functions $g(u)$, and calibrated against the range of finger widths at which the instability is observed experimentally. The function $\kappa(u)$ should admit a spherical cap at the finger tip. It is reasonable to choose this function so that stationary bubbles attached to the tube wall are solutions of the PDE. At zero contact angle, this requires $\kappa(u) = cu^2(1-u)$, with $c > 0$ depending on the form of $g(u)$. At other contact angles, there is a corresponding formula. These changes in the constitutive laws are easily incorporated into both the ODE and PDE solvers, and will be reported on in the future.

**Acknowledgements** Research of the first two authors was funded by NSF grant DMS 0968258. Research of the third author was funded by NSF grant 0968154. Research of the last two authors was funded by a DOE CAREER Award, DE-SC0003907, and a DOE Mathematical Multifaceted Integrated Capability Center, DE-SC0009286.

## References

1. Beresnev I, Gaul W, Vigil RD (2011) Thickness of residual wetting film in liquid–liquid displacement. Phys Rev E 84:026327
2. Bertozzi AE, Münch A, Shearer M (1999) Undercompressive shocks in thin film flows. Physica D 134(4):431–464
3. Blake TD, De Coninck J (2004) The influence of pore wettability on the dynamics of imbibition and drainage. Colloids Surf A 250(1–3):395–402
4. Bretherton FP (1961) The motion of long bubbles in tubes. J Fluid Mech 10:166–188
5. Cueto-Felgueroso L, Juanes R (2012) Macroscopic phase-field model of partial wetting: bubbles in a capillary tube. Phys Rev Lett 108:144502
6. De Lózar A, Juel A, Hazel AL (2008) The steady propagation of an air finger into a rectangular tube. J Fluid Mech 614:173–195

7. Duclaux V, Clanet C, Quéré D (2006). The effects of gravity on the capillary instability in tubes. J Fluid Mech 556:217–226
8. Goren SL (1962) The instability of an annular thread of fluid. J Fluid Mech 12:309–319
9. Scheidegger AE (1974) The physics of flow through porous media. University of Toronto Press, Toronto
10. Taylor GI (1961) Deposition of a viscous fluid on the wall of a tube. J Fluid Mech 10:161–165